Chinese Journal of Chemistry, **2009**, *27*, 1762—1766 **Full Paper**

Apo-CopC and CopC-Cu(II) Unfolding Characteristics in GuHCl Solution

LI, Huiqing(李慧卿) ZHAO, Yaqin(赵亚琴) YANG, Binsheng*(杨斌盛)

Key Laboratory of Chemical Biology and Molecular Engineering of Ministry of Education, Institute of Molecular Science, Shanxi University, Taiyuan, Shanxi 030006, China

The stability of CopC, a copper resistant protein with a Greek β-barrel motif, in GuHCl solution was investigated by fluorescence spectra. Parameter *A*, characterizing position and shape of the fluorescence spectra, "phase diagram" method of fluorescence, and cupric binding capacity in GuHCl solution of different concentration showed that the denaturation transition of apo-CopC and CopC-Cu(II) might be fitted to a simple two-state model. According to a two-state model, the free energy of stabilization for apo-CopC and CopC-Cu(II), (17.08±0.35) and (23.81±0.45) kJ•mol^{-1} respectively, was obtained. Copper(II) increased the stability of apo-CopC. The higher thermodynamics stability of CopC-Cu(II) was revealed to originate in both the faster folding and the slower unfolding rates by unfolding kinetics.

Keywords CopC unfolding, spectral parameter, "phase diagram" method of fluorescence, copper binding capacity, kinetics

Introduction

Proteins often carry out their biological function on the basis of their inherent native fold. Once the native fold was disturbed, protein biological function would be lost to different extent. So the stability has been a problem of outmost interest in biochemistry and biophysics, as was demonstrated by the large literature on this subject.[1-5] Owing to simpler structure of small globular proteins allowing detailed experiments about the effects of various conditions (temperature, ionic strength, pH or concentration of denaturing agents, hydrostatic pressure) on the structure of native molecules,[6-8] these molecules were often used in researching stability of native protein.

The CopC is a soluble protein present in the oxidizing environment of periplasm and is involved in copper trafficking and homeostasis in Gram-negative bacteria.[9,10] The NMR, EXAFS and X-ray crystallographic structure of CopC have been resolved in detail.[11-13] Like cupredoxines and azurin, it exhibits a fold essentially constituted by two β-sheets forming a Greek key β-barrel motif. Two separate but interdependent binding sites, with high specific affinity, one for Cu^{+} and the other for Cu^{2+}, are about 30 Å apart. The aromatic ring of single Trp83, sandwiched between the two β-sheets, locates in a completely hydrophobic environment. In a native state, the CopC protein with other Cop protein (CopABD)[14] functions by sequestering copper ions in the periplasm and exporting the excess without preventing the amount of copper essential for cellular function from reaching the cytoplasm. In this paper, we used spectral parameter A, "phase diagram" method of fluorescence and cupric binding capacity in GuHCl solution of different concentration to explore the stability of apo-CopC and CopC-Cu(II) so as to understand the structural and functional basis of copper resistance. And the role of copper(II) was revealed by comparing CopC-Cu(II) with apo-CopC in thermodynamic stability and in kinetics unfolding experiments.

Experimental

Protein expression and purification

Apo-CopC protein was expressed and isolated with an extra gelfiltration purification step. Negatively charged *E. coli* proteins were removed by passing the lysate supernatant through a DE-52 anion exchange column in 20 mmol•L^{-1} PB buffer at pH 8.0. The flow-through fraction was adjusted to pH 6.0 with 0.2 mol•L^{-1} PB buffer and then applied to a CM cation exchange column in 20 mmol•L^{-1} PB at pH 6.0. The bound proteins were eluted with a salt gradient of 0—0.2 mol•L^{-1} NaCl in 20 mmol•L^{-1} PB. The finally purified proteins were detected by 15% SDS-PAGE and less than 1% Cu content was obtained by atomic absorption spectrum.

Fluorescence measurements

Fluorescence experiments were carried out using an

* E-mail: yangbs@sxu.edu.cn
Received June 18, 2008; revised March 35, 2009; accepted April 30, 2009.
Project supported by the National Natural Science Foundation of China (No. 20771068) and the Natural Science Foundation of Shanxi Province (No. 2007011024).

F-2500 fluorescence spectrophotometer with steady state excitation. Fluorescence was excited at the long wavelength absorption edge where the contribution of tyrosine residues in the bulk protein fluorescence was negligible. The spectrophotometer was equipped with a thermostat that held a constant temperature of 25 ℃ in the cell. The protein concentration was measured spectrophotometrically using molar extinction coefficients at 280 nm of 6970 $L•mol^{-1}•cm^{-1}$. For a thermodynamics experiment, data were recorded after 1 h of incubation of a mixture.

Unfolding kinetics of the protein was initiated by manual mixing of protein solution with 20 $mmol•L^{-1}$ PB buffer (pH 7.0) containing the corresponding amount of GuHCl.

The theory of "phase diagram" method of fluorescence

Any extensive characteristic of the system consisting of two components is determined by the simple equation[15]:

$$I(\theta)=\alpha_1 I_1(\theta)+\alpha_2 I_2(\theta) \quad (1)$$

where I_1 and I_2 are the values of $I(\theta)$ at 100% content of the first and the second components, respectively, and θ_1 and θ_2 are the relative fractions of the components in the system, $\theta_1+\theta_2=1$, and θ is any parameter depending on which content of the components is changed. When two independent extensive characteristics of fluorescence intensity at different emission wavelengths are chosen, we have

$$\begin{aligned} I(\lambda_1)&=\alpha_1 I_1(\lambda_1)+\alpha_2 I_2(\lambda_1) \\ I(\lambda_2)&=\alpha_1 I_1(\lambda_2)+\alpha_2 I_2(\lambda_2) \end{aligned} \quad (2)$$

Eliminating α_1 and α_2 from Eq. (2), we can obtain the relationship between $I(\lambda_1)$ and $I(\lambda_2)$:

$$I(\lambda_1)=a+bI(\lambda_2) \quad (3)$$

where

$$\begin{aligned} a&=I_1(\lambda_1)-\frac{I_2(\lambda_1)-I_1(\lambda_1)}{I_2(\lambda_2)-I_2(\lambda_2)}I_1(\lambda_2) \\ b&=\frac{I_2(\lambda_1)-I_1(\lambda_1)}{I_2(\lambda_2)-I_1(\lambda_2)} \end{aligned} \quad (4)$$

Eq. (3) means that if with the change of fluorescence intensity at two different emission wavelengths the transition between states 1 and 2 follows the model "all-or-none" without formation of the intermediate states,[15] then the parametric relationship between fluorescence intensities at two different emission wavelengths must be linear. If the experimentally recorded fluorescence intensity between two different emission wavelengths of the system is not linear, it unequivocally means that the process of the transition from the initial to the final state is not a one-stage process but proceeds with the formation of one or several intermediate states.

Results and discussion

Two-state model in thermodynamics

Spectral parameter The fluorescence emission maximum of CopC locates near 320 nm owing to its single tryptophanyl residue embedded inside the hydrophobic barrel. After 1 h of incubation under conditions of different GuHCl concentrations, the fluorescence spectra of both apo-CopC and CopC-Cu(II) gradually shifted towards longer wavelength and finally the emission maximum located to 351 nm owing to the exposure to water of the tryptophanyl residue. Comparison of the spectral change from native to unfolded state shows that the greatest differences in fluorescence intensity are in the vicinity of 308 nm for apo-CopC (Figure 1) and 365 nm for CopC-Cu(II) (Figure 2). So the wavelengths 308 and 365 nm were chosen for the registration of intensity change curve for apo-CopC (Figure 1 inset) and CopC-Cu(II) (Figure 2 inset), respectively.

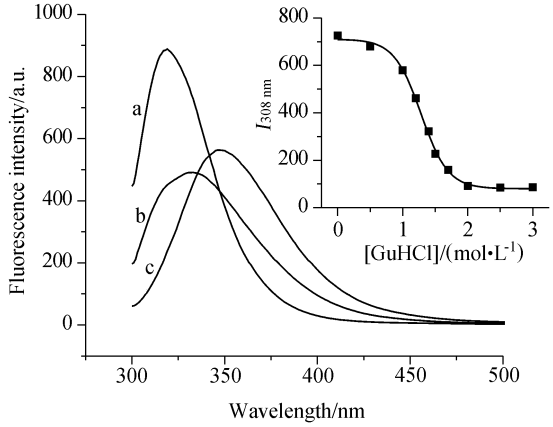

Figure 1 Fluorescence spectra for apo-CopC in different GuHCl concentration ($mol•L^{-1}$): a, 0; b, 1.4; c, 3.5, PB buffer, pH 7.0. Inset is fluorescence intensity change of apo-CopC at 308 nm induced by GuHCl.

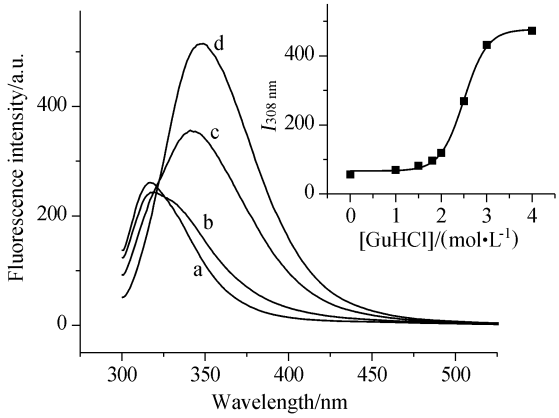

Figure 2 Fluorescence spectra for CopC-Cu(II) in different GuHCl concentration ($mol•L^{-1}$): a, 0; b, 1.8; c, 2.5; d, 3.0, PB buffer, pH 7.0. Inset is fluorescence intensity change of CopC-Cu(II) at 365 nm induced by GuHCl.

The change in the position and shape of the fluorescence spectra with increasing GuHCl concentration was also studied. For the purpose, the changes in ratio of the intensities at two different wavelengths which were chosen from two different slopes of the spectrum, the so-called spectral parameter $A=I_{308\ nm}/I_{365\ nm}$ was used[16]. Figure 3 represents the dependence of parameter *A* value on the concentration of GuHCl. In order to compare apo-CopC with CopC-Cu(II), the same standard for *A* was chosen. It can be seen that in the unfolding process the position and shape of the fluorescence spectra of both apo-CopC and CopC-Cu(II) present a sigmoidal change, according with the fluorescence intensity tendency. The conformational transition of both apo-CopC and CopC-Cu(II), thus, may be fitted to a simple two-state model.

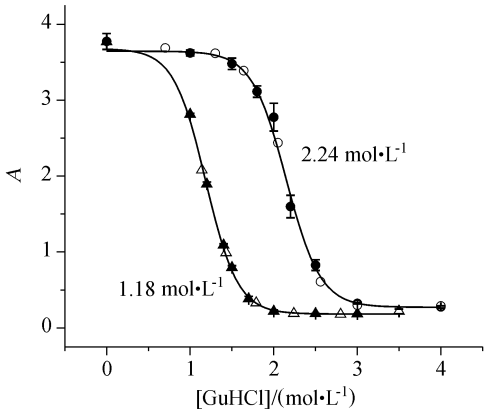

Figure 3 Denaturation (solid symbols) and renaturation (open) profiles of apo-CopC (triangles) and CopC-Cu(II) (circles) according to normalized spectral parameter *A* in PB buffer, pH 7.0.

The renaturation of apo-CopC and CopC-Cu(II) was also performed by suitable dilution of fully unfolded samples. A complete recovery of all the native spectroscopic features was observed. The recovery of the fluorescence features reflected by data recorded at 308 and 365 nm is coincident with the curve of the unfolding apo-CopC or CopC-Cu(II) from the corresponding data, suggesting completely reversible denaturation process.

"Phase diagram" method of fluorescence The analysis of the protein conformational transition based on the construction of a parametric relationship between the fluorescence intensities recorded at two different wavelengths for apo-CopC and CopC-Cu(II) was also performed.[15,17,18] The wavelengths of 308 and 365 nm according to experience were used as independent characteristics parameters. It was found that the linearity of the parametric relationship in accordance with the Eq. (3) between $I_{308\ nm}$ and $I_{365\ nm}$ for the two proteins (Figure 4A and 4B) existed, which indicates that the denaturation of apo-CopC and CopC-Cu(II) induced by GuHCl obeys a typical two-state model and there was only one conformational transition from the native to the unfolded state during the unfolding process.

Copper binding capacity As a copper resistance protein, binding copper(II) is specific for apo-CopC in the native fold, which is exhibited by significantly quenching fluorescence intensity of the protein until the ratio of $[Cu^{2+}]/[\text{apo-CopC}]=1.0$.[19] Once it unfolds, no copper(II) would be bound, or copper(II) would not affect on fluorescence emission of apo-CopC. If there are only native apo-CopC and unfolding states during the denaturation process, the capacity of copper(II) binding would be decided only by the fraction of protein keeping the native fold. Thus copper(II) binding would bring linear fluorescence quenching just as in the absence of GuHCl. So this method can also be used to determine the fraction of the native protein in a two-state denaturation. Figure 5 shows normalized fluorescence titration curves of copper(II) to apo-CopC at the different concentrations of GuHCl. As can be seen, the linear fluorescence quenching occurs at any certain concentration of GuHCl. Regarded as standard in the absence of GuHCl, fluorescence quenching decreases with increaseing concentration of GuHCl.

The copper(II) binding fraction of apo-CopC in different concentrations of GuHCl can be directly obtained by the observable mole ratio of Cu^{2+} to apo-CopC. The change of copper(II) binding induced by increasing GuHCl is of also a sigmoidal shape. For a

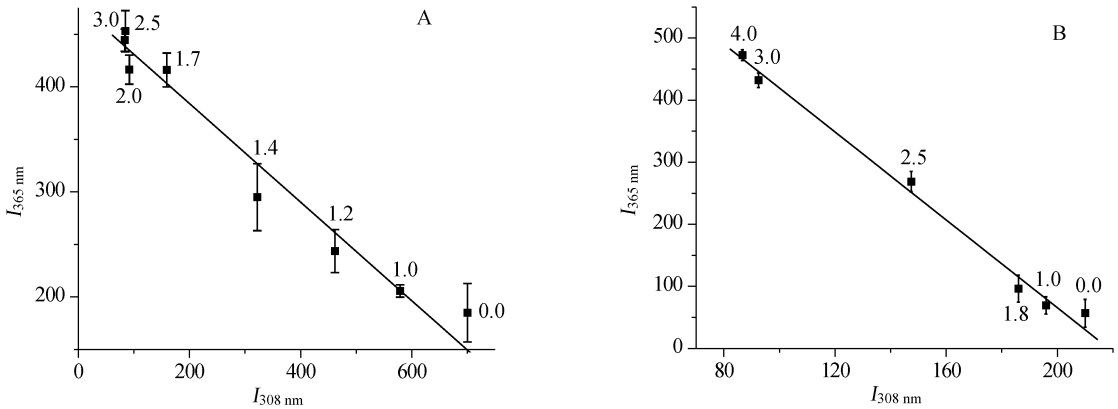

Figure 4 Phase diagram of fluorescence representing the unfolding of apo-CopC (A) and CopC-Cu(II) (B) induced by an increase in GuHCl concentration. The values on the line are the concentration of GuHCl (mol•L^{-1}).

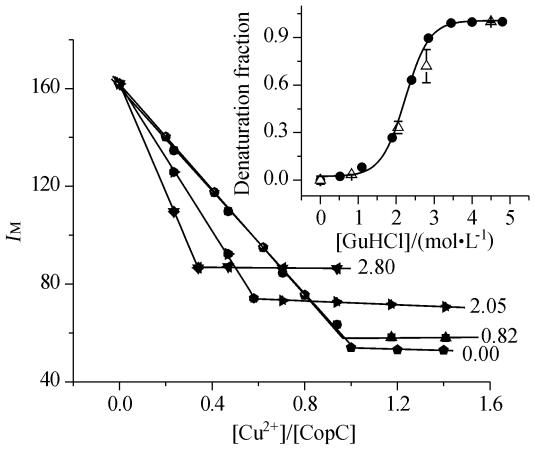

Figure 5 Titration curve of copper to apo-CopC in the presence of GuHCl at different concentrations (mol•L^{-1}). Inset showed denaturation fraction profiles of CopC-Cu(II) obtained according to copper binging fraction (open triangles) and spectral parameter (solid circles).

reversible equilibrium, the denaturation fraction from a copper(II) titration experiment should agree with that from denaturizing CopC-Cu(II). Comparing the denaturation fraction profile (Figure 5 inset) from the experiment with that from spectral parameter *A*, the tendency is almost consistent. And the denaturant concentrations at the midpoint of the transition yields from the experiment are in accordance with those from spectral parameter *A*.

Gibbs free energy

For a two-state equilibrium, the equilibrium constant is given according to the ratio of the fraction of the unfolding to native protein. Further we can obtain the Gibbs free energy $\Delta G^{\ominus}$ for different [GuHCl] and $\Delta G^{\ominus}_{H_2O}$ for the folding process in pure water from the intercept of a plot of $\Delta G^{\ominus}$ versus [GuHCl]. According to the data from Figure 3, the Gibbs free energy of apoCopC and CopC-Cu(II) was calculated to be (17.08 $\pm$0.35) and (23.81$\pm$0.45) kJ•mol^{-1}, respectively. The data reveal a distinctly higher structural stability of CopC-Cu(II).

Unfolding kinetics

The equilibrium experiments clearly show that unfolding is reversible and it proceeds with apparent two-state behavior. The stability for apo-CopC decreases as compared to CopC-Cu(II). To reveal whether the increased thermodynamic stability of CopC-Cu(II) originates in either the folding or the unfolding rates, or both, the kinetics of CopC unfolding induced by GuHCl of different concentrations was studied. Comparison of the spectral change during the unfolding process shows that the greatest differences in fluorescence intensity are in the vicinity of 308 nm for apo-CopC and 365 nm for CopC-Cu(II). In order to observe distinctly, thus, the fluorescence intensity change at 308 nm for apo-CopC and 365 nm for CopC-Cu(II) over time was recorded. It can be inferred from "phase diagram" of fluorescence (Figure 4A and Figure 4B) that the fluorescence intensity change at both wavelengths is synchronous for each protein, thereby data chosen from different wavelengths for the two proteins would not affect the experiment results. Figure 6 are the profiles of unfolding apo-CopC (A) and CopC-Cu(II) (B), from which it can be seen that at any certain concentration of GuHCl, the fluorescence intensity changes monotonically with time, finally approaching its equilibrium value. The unfolding kinetics follows the two-state behavior. In addition, the unfolding equilibrium can be attained by incubating the protein for 1 h at any concentration of GuHCl and the equilibrium experiments are dependable.

The data are successfully fitted to a single exponential function. In Figure 7, we show the natural logarithm of the unfolding rate constants obtained under pseudo-first-order conditions for CopC-Cu(II) and apo-CopC as a function of denaturant concentration. The logarithms of the rate constants for apo-CopC and CopC-Cu(II) depend linearly on the denaturant concentration. Thus, unfolding rate constants in the absence of the denaturant were obtained by measuring the unfolding rate at different GuHCl concentrations and extrapolating to 0 mol•L^{-1}.[20,21] Apparently CopC-Cu(II) unfolded more slowly than apo-CopC at any denaturation concentration and CopC-Cu(II) is kinetically more stable than apo-CopC.

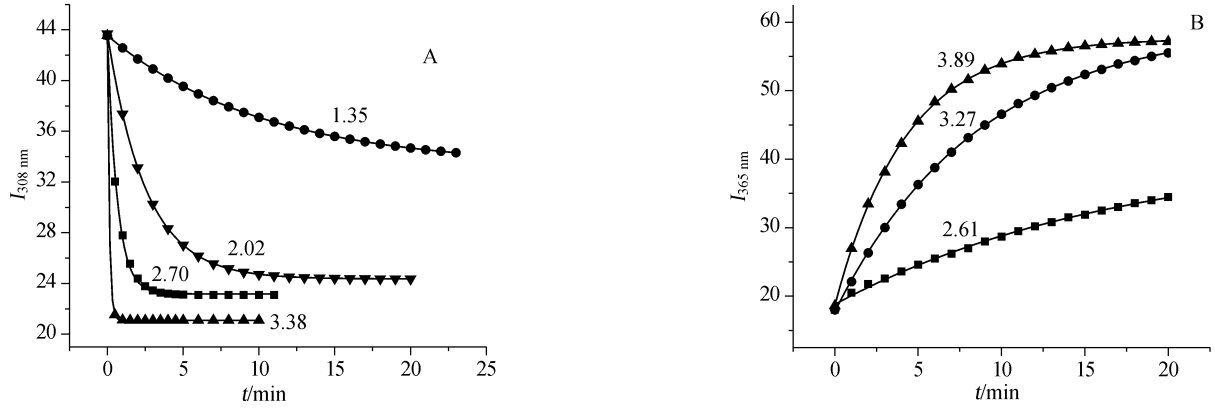

Figure 6 Kinetics of apo-CopC (A) and CopC-Cu(II) (B) denaturation monitored by the change of intrinsic fluorescence intensity at 308 nm (A) and 365 nm (B), respectively. The values on the curves are the concentrations of GuHCl (mol•L^{-1}).

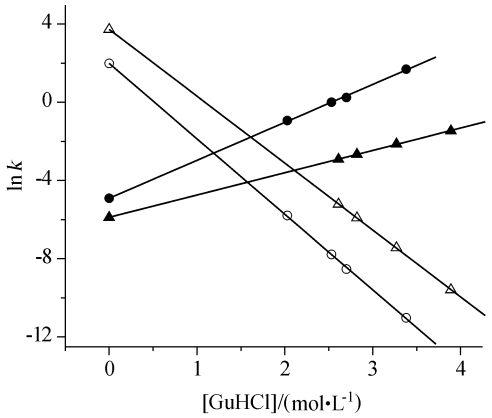

Figure 7 Natural logarithm of unfolding (solid) and folding (open) rate constants for CopC-Cu(II) (traingles) and apo-CopC (circles) as a function of GuHCl concentration. The natural logarithm of the unfolding rate constants for CopC-Cu(II) and apo-CopC in the absence of GuHCl was obtained by extrapolating to 0 mol•L^{-1} GuHCl.

Then, we used the unfolding rate constants and the equilibrium constants from the experiment above-mentioned to calculate the folding speed constants for CopC-Cu(II) and apo-CopC at each denaturant concentration. The Chevron plot is also displayed in Figure 7, which shows that the fold rate constants increase linearly as the denaturant concentrations decreases for both proteins. Copper(II) increases the fold rates of apo-CopC. By comparing the unfold and fold rates of apo-CopC with CopC-Cu(II) in the absence of GuHCl, the mechanism by which Cu(II) stabilizes the native form of apo-CopC can be attributed both to a deceleration of unfolding and to an acceleration of refolding.

Acceleration of refolding or (and) deceleration of unfolding is a general property of native-state stabilization of cofactors binding proteins. A 13-residue peptide, derived from the β-barrel protein azurin, was reported to adopt a β-hairpin structure in solution upon copper ligation, which indicates that the metal ligand region of azurin may act as the nucleation site that, upon copper coordination, directs (and possibly speeds up) the folding.[22] *R*-lactalbumin was found to refold more quickly in the presence of metals.[23,24] It was also observed in our experiment of copper(II) titration of apo-CopC in different concentration denaturant that red-shifted emission maximum recovered partially. A few studies targeting the effect of cofactors on folding found that calcium ions stabilized RNase HI and staphylococcal nuclease A proteins by decreasing the unfolding speed.[25] Our experiments demonstrate that binding copper(II) protects the native-state of CopC toward solvent perturbations and copper(II) promotes refolding of CopC.

References

1 Catanzano, F.; Graziano, G.; Paola, B. D.; Barone, G. *Biochemistry* **1998**, *37*, 14484.
2 Dragani, B.; Cocco, R.; RidderstrÖm, M.; Stenberg, G.; Mannervik, B.; Aceto, A. *J. Mol. Biol.* **1999**, *291*, 481.
3 Zheng, X. Y.; Pang, E. G.; Li, H. Q.; Zhao, Y. Q.; Yang, B. S. *Chinese. J. Chem.* **2007**, *25*, 630.
4 Zheng, X. Y.; Pang, E. G.; Li, H. Q.; Zhao, Y. Q.; Yang, B. S. *Chin. Sci. Bull.* **2007**, *52*, 743.
5 Chang, J. Y.; Li, L. *FEBS Lett.* **2002**, *511*, 73.
6 Mei, G.; Venere, A. D.; Campeggi, F. M.; Gilardi, G.; Rosato, N.; Matteis, F. D.; Finazzi-Agrò, A. *Eur. J. Biochem.* **1999**, *265*, 619.
7 Cioni, P.; Bramanti, E.; Strambini, G. B. *Biophys. J.* **2005**, *88*, 4213.
8 Fuentes, L.; Oyola, J.; Fernandez, M.; Quinones, E.; Fuentes, L.; Oyola, J.; Fernandez, M.; Quinones, E. *Biophys. J.* **2004**, *87*, 1873.
9 Cooksey, D. A. *FEMS Microbiol. Rev.* **1994**, *14*, 381.
10 Silver, S. *Gene* **1996**, *179*, 9.
11 Zhang, L. Y.; Koay, M.; Maher, M. J.; Xiao, Z. G.; Wedd, A. G. *J. Am. Chem. Soc.* **2006**, *128*, 5834.
12 Arnesano, F.; Banci, L.; Bertini, I.; Felli, I. C.; Luchinat, C.; Thompsett, A. R. *J. Am. Chem. Soc.* **2003**, *125*, 7200.
13 Arnesano, F.; Banci, L.; Bertini, I.; Thompsett, A. R. *Structure* **2002**, *10*, 1337.
14 Mellano, M. A.; Cooksey, D. A. *J. Bacteriol.* **1998**, *170*, 2879.
15 Kuznetsova, I. M.; Stepanenko, O. V.; Stepanenko, O. V.; Povarova, O. I.; Biktashev, A. G.; Verkhusha, V. V.; Shavlovsky, M. M.; Turoverov, K. K. *Biochemistry* **2002**, *41*, 13127.
16 Turoverov, K. K.; Verkhusha, V. V.; Shavlovsky, M. M.; Biktashev, A. G.; Povarova, O. I.; Kuznetsova, I. M. *Biochemistry* **2002**, *41*, 1014.
17 Jiao, M.; Liang, Y.; Li, H. T.; Wang, X. *Acta Chim. Sinica* **2003**, *61*, 1362 (in Chinese).
18 Yang, F.; Liang, Y.; Yang, F. *Acta Chim. Sinica* **2003**, *61*, 803 (in Chinese).
19 Li, H. Q.; Zheng, X. Y.; Pang, E. G.; Zhao, Y. Q.; Yang, B. S. *Spectrochim. Acta, Part A* **2008**, *70*, 384.
20 Manning, M.; Colon,W. *Biochemistry* **2004**, *43*, 11248.
21 Pozdnyakova, I.; Guidry, J.; Wittung-Stafshede, P. *Arch. Biochem. Biophys.* **2001**, *390*. 146.
22 Pozdnyakova, I.; Guidry, J.; Wittung-Stafshede, P. *J. Am. Chem. Soc.* **2000**, *122*, 6337.
23 Sugawara, T.; Kuwajima, K.; Sugai, S. *Biochemistry* **1991**, *30*, 2698.
24 Goedken, E. R.; Keck, J. L.; Berger, J. M.; Marqusee, S. *Protein Sci.* **2000**, *9*, 1914.
25 Kuwajima, K.; Mitani, M.; Sugai, S. *J. Mol. Biol.* **1989**, *206*, 547.

(E0806184 Cheng, F.)